

Chauffeur braking

Problem presented by

Phil Barber and Huw Williams

Jaguar Land Rover

Executive Summary

An experienced driver will ‘feather’ the brakes so as to unwind the suspension compliance and stop the vehicle with only just enough torque in the brakes to hold the vehicle stationary on any gradient, or against the residual torque from an automatic transmission’s torque converter. An optimal stopping problem that minimises the total jerk was formulated and solved. This model was extended by including a linear relationship between the brake pressure and the acceleration of the car where the coefficients are estimated by linear regression. Finally, a Kalman filter estimates the state of the car using the tone wheel.

Version 4.0
11 June 2009

Report author

Tristram Armour (Industrial Mathematics KTN)

Contributors

David Allwright (Industrial Mathematics KTN)
Tristram Armour (Industrial Mathematics KTN)
Chris Cawthorn (University of Cambridge)
Chris Dent (University of Edinburgh)
Jeff Dewynne (University of Oxford)
Joseph Fehribach (WPI)
Gemma Fay (University of Oxford)
John Lees-Miller (University of Bristol)
Jan Van lent (University of Bath)
Jonathan Ward (University of Limerick)
Robert Whittaker (University of Oxford)

ESGI68 was jointly organised by
The University of Southampton
The Knowledge Transfer Network for Industrial Mathematics

and was supported by
The Engineering and Physical Sciences Research Council

Contents

1	Introduction	1
1.1	Problem Description	1
2	Optimising comfort	1
2.1	Problem Formulation	1
2.2	Solution	3
2.3	Discussion	6
3	Optimal control framework	7
3.1	State estimation	7
3.2	Braking pressure model	10
3.3	The control strategy	10
4	Conclusions	11
4.1	Remarks	11
4.2	Friction	12
4.3	Suggested further research	13
5	Appendix	13
5.1	Derivation of the Euler–Lagrange Equations	13
5.2	Analysis of the optimisation problem (continued)	14
5.3	An aside on self-similar stopping profiles	17
5.4	Friction Models: Canudas de Wit Model	18
5.5	Friction Models: Combined Coulomb, Stribeck, viscous, Dankowicz Model	19
6	Bibliography	19
6.1	Friction references	19

1 Introduction

1.1 Problem Description

- (1.1.1) An experienced driver will ‘feather’ the brakes so as to unwind the suspension compliance and stop the vehicle with only just enough torque in the brakes to hold the vehicle stationary on any gradient, or against the residual torque from an automatic transmission’s torque converter. Once stationary, the brake pressure can be increased significantly to hold the vehicle against disturbances. The problem offered to the Study Group is to provide a comfortable ‘chauffeur’ stop feature for a luxury vehicle under full automatic longitudinal control.
- (1.1.2) Four main parts to the problem were identified.
- (a) Optimal control: Braking control must take account of initial conditions, end conditions and possible disturbances.
 - (b) State estimation: Vehicle movement is detected by a ‘tone wheel’ attached directly to each of the vehicle’s road wheels. The tone wheel has teeth that generate square waves in Hall-effect sensors, which are then used to estimate vehicle speed. There are virtually no other sensors available.
 - (c) Friction braking: The classical model of friction has sliding and static elements. Brake materials are both adhesive and abrasive and contain lubricants such as aluminium. Are there better (micro-molecular) models at the stick-slip boundary?
 - (d) Braking dynamics: There is an unknown and changing offset and gain in the (open loop) brake pressure control, owing to the brake disk condition and the effects of gradient, engine braking and torque converter creep.

The Study Group concentrated on the first three problems following advice from Phil Barber.

2 Optimising comfort

2.1 Problem Formulation

- (2.1.1) First of all, we need to define what is meant by a comfortable stop. For a comfortable stop, Jaguar suggested that the magnitude of the acceleration should be less than 3 m/s^2 and the jerk (or change in acceleration) should be less than 1 m/s^3 . However, the main cause of discomfort is the jerk so as long as the acceleration is not too large, we wish to minimise the jerk.
- (2.1.2) We define the *discomfort* J in terms of the velocity profile $v(t)$ over the stopping period $0 < t < T$ by

$$J[v, T] = \int_0^T (\ddot{v})^2 dt, \quad (1)$$

and assume that the smoothest ride is given by the trajectory $v(t)$ that minimises J . We wish to stop the car as smoothly as possible, bringing it to rest in a distance D from an initial velocity $v(0) = v_0$ and acceleration $\dot{v}(0) = a_0$. There are of course, other ways we could define the discomfort of a car coming to stop but the time intergral of the jerk squared is what we looked at during the week.

- (2.1.3) We non-dimensionalise distances on D and times on D/v_0 . So the velocity and acceleration scales are v_0 and v_0^2/D respectively. There is a single non-dimensional parameter in the problem, which describes the initial acceleration

$$\alpha = \frac{a_0 D}{v_0^2}. \quad (2)$$

We also introduce a non-dimensional stopping time $\tau = v_0 T/D$, in terms of the real stopping time T . Since T is unknown, τ must be determined as part of the solution.

- (2.1.4) We wish to minimise the dimensionless discomfort, $J[v, \tau]$ with respect to variations in the velocity profile $v(t)$ and the stopping time τ , subject to the following conditions:

- (a) The car starts from the given initial conditions at $t = 0$:

$$v(0) = 1, \quad \dot{v}(0) = \alpha. \quad (3)$$

- (b) The car comes to a halt at $t = \tau$, and also has no acceleration at this point. (For otherwise there would be an infinite jerk as the acceleration instantaneously jumps to zero for $t > \tau$.)

$$v(\tau) = 0, \quad \dot{v}(\tau) = 0. \quad (4)$$

- (c) The car stops at the required distance from its initial location

$$\int_0^\tau v(t) dt = 1. \quad (5)$$

- (d) The car never has to reverse:

$$v \geq 0. \quad (6)$$

- (e) We may also want to consider further restrictions, such as positive acceleration never occurring once braking has begun, and the stopping point being reached within a specified time.

- (2.1.5) We introduce a Lagrange multiplier λ for the integral constraint (5) in the usual way, and hence the minimisation problem is expressed as

$$\text{minimise } I[v, \tau] = \int_0^\tau (\ddot{v})^2 - \lambda v \, dt, \quad (7)$$

with respect to variations in $v(t)$ and τ , subject to $v(t) \geq 0$ and

$$v(0) = 1, \quad \dot{v}(0) = \alpha, \quad v(\tau) = 0, \quad \dot{v}(\tau) = 0, \quad \int_0^\tau v(t) \, dt = 1. \quad (8)$$

2.2 Solution

- (2.2.1) In appendix 5.1, we derive the appropriate Euler–Lagrange equations for a system of the type (7)–(8). From (29), we find that $v(t)$ must satisfy

$$\frac{d^4 v}{dt^4} = \frac{1}{2} \lambda \quad \text{for } 0 < t < \tau, \quad (9)$$

for I to be minimal with respect to variations in $v(t)$. The condition (30) implies

$$\frac{d^2 v}{dt^2} = 0 \quad \text{at } t = \tau, \quad (10)$$

for I to be minimal with respect to variations in τ .

- (2.2.2) Equations (9) and (10) apply only at points where $v > 0$. At points where $v = 0$ the constraint $v \geq 0$ restricts the permitted variations. In the interior we may find solutions which are piecewise quartic polynomials, but have a discontinuity in $\ddot{v}(t)$ at points where $v = 0$. At the end-point, the boundary conditions mean that the point where $v \geq 0$ is about to be broken occurs when $\ddot{v}(\tau) = 0$, so condition (10) always applies.

- (2.2.3) Setting aside the $v \geq 0$ constraint for the time being, we see that (9) implies that $v(t)$ must be a quartic polynomial in t . The five conditions (8) uniquely determine the coefficients in terms of α and τ . We obtain

$$v(t) = A(\tau - t)^2 + B(\tau - t)^3 + C(\tau - t)^4, \quad (11)$$

where

$$A = -\frac{3(\alpha\tau^2 + 8\tau - 20)}{2\tau^3}, \quad (12)$$

$$B = \frac{4(\alpha\tau^2 + 7\tau - 15)}{\tau^4}, \quad (13)$$

$$C = -\frac{5(\alpha\tau^2 + 6\tau - 12)}{2\tau^5}, \quad (14)$$

and $\lambda = 48C$.

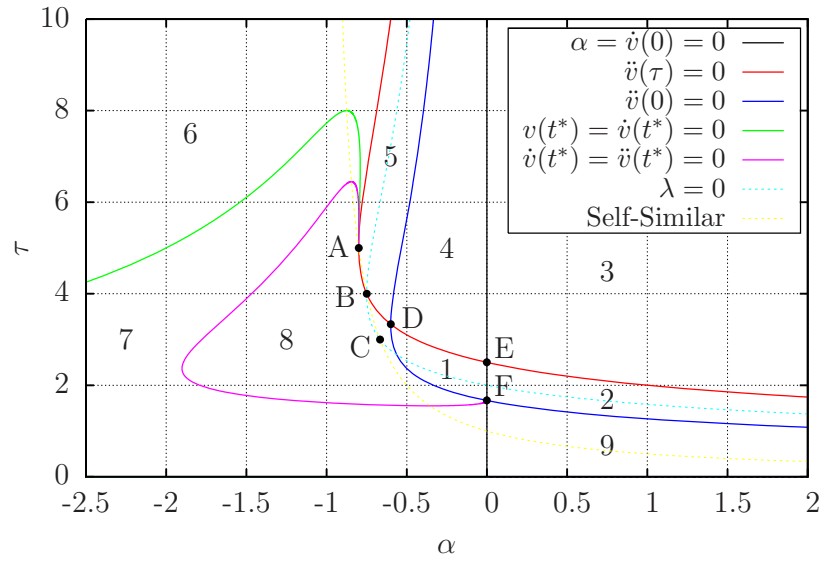


Figure 1: A plot of the α - τ plane. Each point in the plane corresponds to a stopping profile that minimises J subject to the given stopping distance and time. The solid lines separate the numbered regions 1–9 in which the solutions have different characteristics. Intersections of interest are labelled with the letters A–F.

- (2.2.4) Figure 1 shows a plot of the α - τ plane. Each point corresponds to a polynomial (11) that minimises I with respect to variations in v (but not necessarily with respect to variations in τ). The lines divide solutions with different characteristics. Sketches of these different types of solutions are shown in figure 2.
- (2.2.5) Only those in regions 1, 2 and 8 are physically reasonable. The others involve either an increase in acceleration before braking begins, a region of negative velocity (reversing) or a region of acceleration after some initial braking.
- (2.2.6) We must now consider how to choose an optimal solution for each α , by selecting appropriate stopping time τ . The solution may be a single polynomial, or made up of two or more polynomials that are followed for different time intervals (the transitions occurring at points where the constraint $v \geq 0$ is only just satisfied).
- (2.2.7) The rest of the analysis can be followed in the Appendix in section 5.2. In the end, the solution can be divided into two cases:

Case 1: $\alpha \equiv a_0 D / v_0^2 \geq -3/4$

In this case we adopt the single-phase solution, given by the polyno-

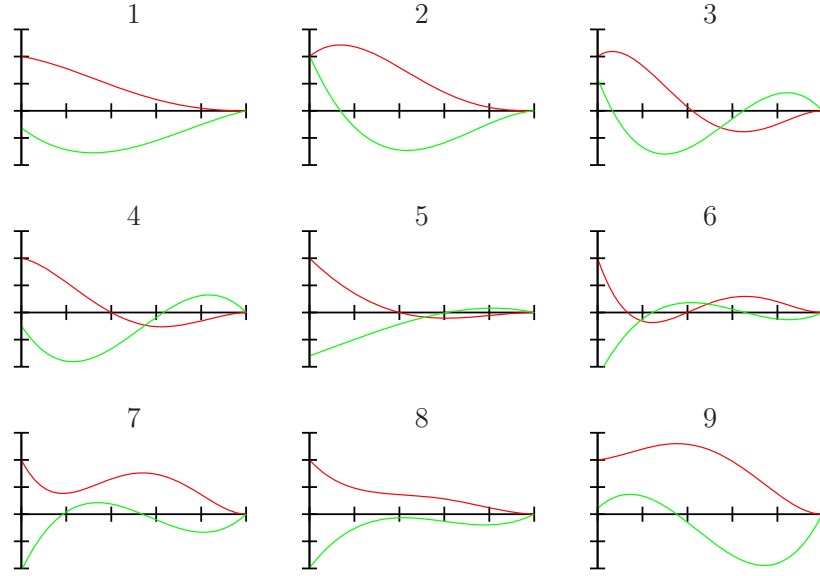


Figure 2: Plots for the various characteristic solution types occurring in the different regions in figure 1. Time is on the horizontal axis. Red lines show the velocity $v(t)$, and green lines the acceleration $\dot{v}(t)$.

mial (11) with τ set by the condition (32). This results in

$$v(t) = (4 + 2\alpha\tau) \left(1 - \frac{t}{\tau}\right)^3 - (3 + 2\alpha\tau) \left(1 - \frac{t}{\tau}\right)^4, \quad (15)$$

$$\tau = \frac{5}{1 + \sqrt{1 + 5\alpha/4}}. \quad (16)$$

In figure 1, these solutions lie on the red line, at and to the right of point B.

Case 2: $\alpha \equiv a_0 D / v_0^2 < -3/4$

Here the optimal solution comprises two phases. We first come to rest in a shorter distance, before inching forwards arbitrarily slowly to arrive at the required stopping point in an infinite time. The first phase of the motion is given by an appropriate rescaling of the solution at point B of figure 1. We have

$$v(t) = \left(1 - \frac{t}{t^*}\right)^3, \quad (17)$$

for $0 < t < t^*$, where

$$t^* = -\frac{3}{\alpha}. \quad (18)$$

The distance covered in this time is

$$d_1 \equiv \int_0^{t^*} v(t) dt = -\frac{3}{4\alpha} < 1. \quad (19)$$

- (2.2.8) Observe that the solutions for both cases converge to the same trajectory (namely the solution corresponding to point B of figure 1) as $\alpha \rightarrow -4/3$. The full stopping profiles corresponding to points B and E in Figure 2 are shown in Figures 3 and 4.

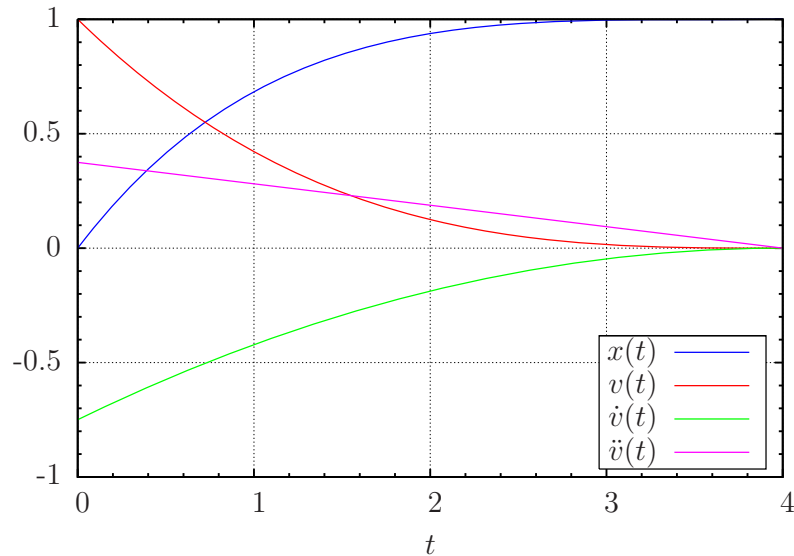


Figure 3: The dimensionless displacement, velocity, acceleration and jerk as functions of time, for optimal braking from an initial acceleration $\alpha = -3/4$. This corresponds to point B on figure 1.

2.3 Discussion

- (2.3.1) Case 1 corresponds to a normal stopping event, and should be relevant to most situations where stopping is required to occur. Case 2 corresponds to an ‘over-breaking’ situation in which the car is already breaking too rapidly given the required stopping distance. This is only likely to occur in situations where the car was attempting to stop at a certain point and then the situation changes and the stopping point is moved further ahead of the car. Examples of this might include a red traffic light ahead turning green, or a stationary car waiting to turn right making the turn and clearing the road. In both cases, there could be another reason to stop further along the road.

- (2.3.2) Physically the optimal solution of crawling along infinitely slowly is not much use. There are two sub-cases to consider:

Case 2a : The natural stopping point at $d_1 = -3/(4\alpha)$ is close enough to the required point, that it doesn’t matter. In which case, the car should just adopt the first phase of the stopping trajectory and not attempt to cover the remaining distance.

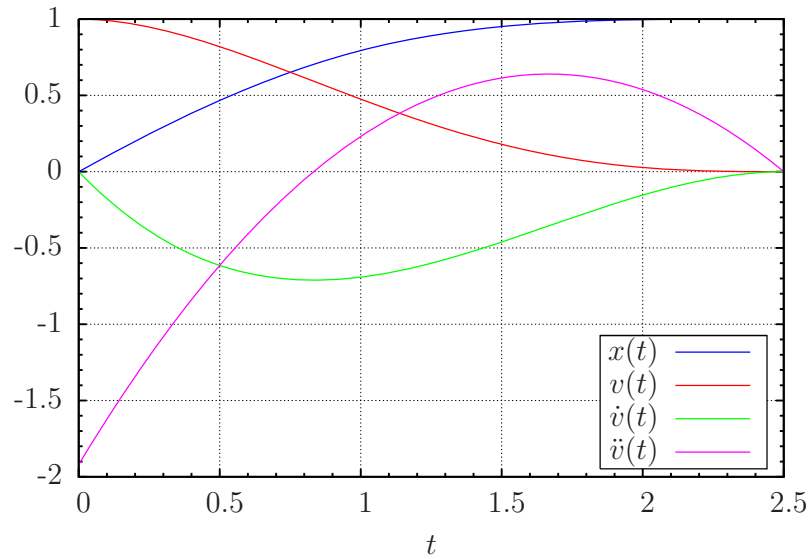


Figure 4: The dimensionless displacement, velocity, acceleration and jerk as functions of time, for optimal braking from an initial acceleration $\alpha = 0$. This corresponds to point E on figure 1.

Case 2b : The natural stopping point at d_1 is a significant distance before the required stopping point. In this case the desired option is likely to be to come out of the deceleration, continue at some “optimal” speed for the road conditions for some time, and then execute a stopping manoeuvre from a closer point. Apart from a possible large initial jerk coming out of the deceleration (which is pretty much unavoidable) the rest of the manoeuvre will hopefully be sufficiently smooth that it doesn’t matter that the jerk is not strictly minimised. In this case, we are not initially in a ‘stopping regime’ and it is the responsibility of the regular driving control system to determine appropriate car speed behaviour until the braking begins.

3 Optimal control framework

3.1 State estimation

(3.1.1) Any optimal stopping problem will require that we know the initial state of the car. In reality, our model will be imperfect and so due to model and parameter uncertainties, we will need to update our optimal control as the car brakes. If we had accurate sensors available each feeding a time series of information to the control system, this might not be such a problem but the cars have limited bandwidth and space for sensors. The Study Group concentrated on a solution with the speed sensor only. The control strategy is to use the estimates of the current state of the

vehicle to determine how to adjust the braking system of the car in order to affect a smooth stop, following an appropriate optimal stopping profile from Section 2.

- (3.1.2) A Hall-effect sensor together with a tone wheel acts as a speed sensor for the car. The tone wheel is a cog with 48 square teeth (see Figure 5) and each revolution of the tone wheel corresponds to the car moving 2.101 metres. The velocity is calculated by looking at the time taken until the next tooth of the cog passes the sensor. The teeth are imperfect so there will be some error to the velocity calculation which increases when the car is moving very slowly.

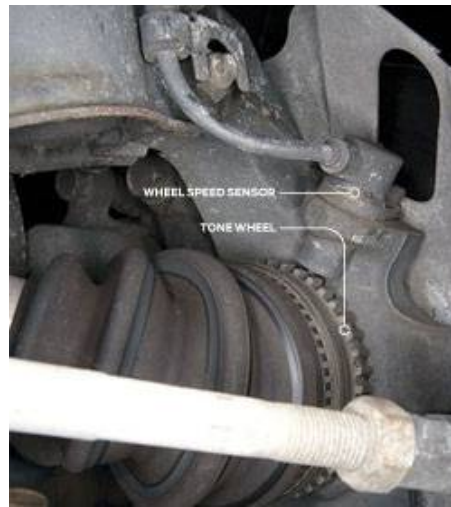


Figure 5: Picture of a tone wheel. (Courtesy of eHow.com)

- (3.1.3) The solution method here is a Kalman filter which will provide state estimates of the car in between updates from the speed sensor. Let x_t be the state of the car at time t . The Kalman filter assumes we have a linear dynamical system hence the true state of the system at time t , x_t , satisfies

$$x_t = Fx_{t-1} + Bu_{t-1} + w_{t-1} \quad (20)$$

where u_t is the control applied to the system at time t and w_t is the process noise at time t which is modelled by Gaussian white noise with covariance Q_t . At each time step an observation of the true state, z_t , is made which satisfies

$$z_t = Hx_t + v_t \quad (21)$$

where v_t is the observational noise modelled by Gaussian white noise with covariance R_t .

(3.1.4) For the simplified problem with no friction, we have for dt ‘small’

$$\begin{aligned} x_t &= \begin{pmatrix} x \\ \dot{x} \end{pmatrix} & F &= \begin{pmatrix} 1 & dt \\ 0 & 1 \end{pmatrix} & H &= \begin{pmatrix} 0 & 0 \\ 0 & h(t) \end{pmatrix} \\ B &= \begin{pmatrix} 0 & 0 \\ dt & 0 \end{pmatrix} & u_t &= \begin{pmatrix} a_t \\ 0 \end{pmatrix} \end{aligned} \quad (22)$$

where $h(t) = 0$ when the tone wheel at time t is currently undetected by the sensor, otherwise $h(t) = 1$. a_t is the optimal acceleration calculated by the control system at time t .

(3.1.5) A simple simulation of the stopping problem with a tone wheel (with simulated errors) was made. At each time step, the Kalman filter gave the control system estimates of the state of the car. The control system calculates the solution to the problem in section 2.1 for the next time step until the car comes to a stop. Figure 6 shows the last section of the simulation. The jumps in the curves indicate where new measurements were received from the tone wheel and these updates become less frequent as the vehicle slows down. The shaded area is 1 standard deviation away from our estimate and our real position is within the shaded area for the whole simulation.

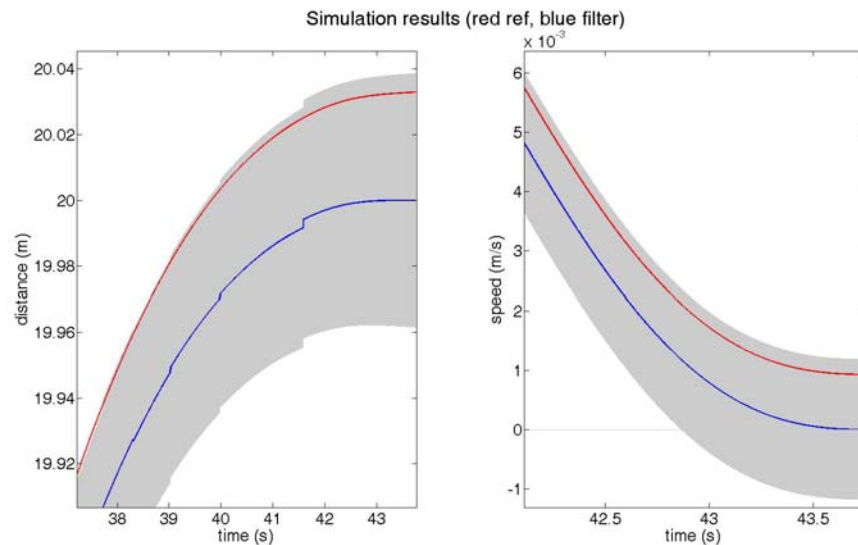


Figure 6: Simulation results using the Kalman filter: The left graph shows the actual (red) and detected displacement (blue) of the car from the start point at 0 metres. The stopping distance was set at 20 metres. The right graph plots the speed of the car at the end of the simulation. The optimal stop took approximately 43 seconds.

(3.1.6) Remarks:

- Strictly, the errors come from the timings of the updates and not from the readings themselves. However, the Kalman filter is designed to operate in the presence of noise and hence it is very robust — it should still work well in our problem.
- Because of the design of the sensor and the lack of an accurate accelerometer, the control system doesn't really know if the car has stopped. There is the need for a higher level control system which increases the brake pressure when an update has not occurred for s seconds, at which the car assumes you have stopped.

3.2 Braking pressure model

- (3.2.1) In reality, the control available to the chauffeur is the braking pressure and not the acceleration of the car. The relationship between the two depends on the gradient of the road, the brake condition, the coefficient of friction, mass of the car and perhaps other parameters that are unknown to the control system. This can all be approximated by a linear relationship

$$\ddot{x} = \delta + \gamma p + \epsilon \quad (23)$$

where p is the braking pressure, γ and δ are constants and ϵ is an error term. Assuming ϵ is zero-mean Gaussian, we can use linear regression to estimate γ and δ using the state estimates from the Kalman Filter.

- (3.2.2) This model assumes we have simple sliding friction only. If after tests we see that the stick-slip boundary needs to be examined further, there are some more sophisticated friction models in the Appendix in sections 5.4 and 5.5.

3.3 The control strategy

- (3.3.1) We updated the control strategy taking into account the tone wheel and the linear braking pressure model. A diagram for the algorithm can be seen in Figure 7. At each time step, the state of the car is estimated and an optimal acceleration is calculated. At the same time, the past braking pressure and acceleration data will be used to estimate the braking pressure model parameters. This is then combined to find the optimal braking pressure for the car. This continues until the car is estimated to have stopped by the Kalman filter. Unfortunately, there was no time during the Study Group week to write a complete set of code to test this framework.

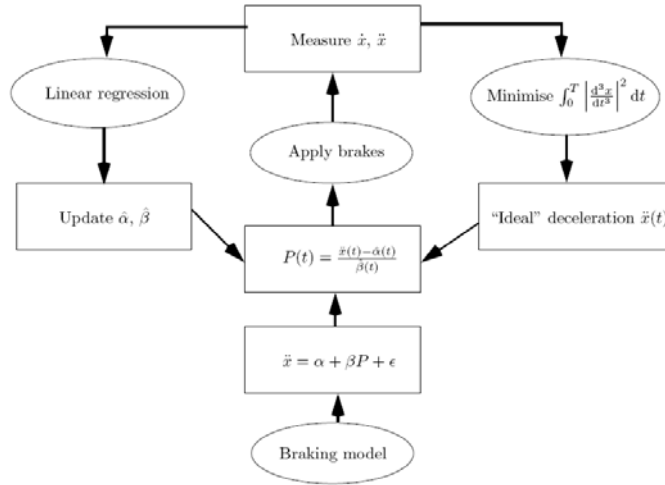


Figure 7: Proposed optimal control strategy

4 Conclusions

4.1 Remarks

- (4.1.1) When considering the ideal stopping trajectory, one should look at the overall value of the discomfort, and the peak jerk. If these are lower than some defined thresholds, it probably means you don't need to start stopping yet. You can continue at your current speed or what ever the road conditions dictate (to arrive as quickly as possible) or possibly release the accelerator to begin slowing down gradually (in order to save fuel and brakes). The stopping procedure begins at some later point, determined by when the optimal trajectory starts to exceed the set discomfort thresholds.
- (4.1.2) While we chose to minimise the integral of jerk-squared, it is possible that this could have lead to large peak values over small time-intervals – which wouldn't be physically desirable. However, this is found not to be the case, as the solutions are all smooth polynomials, and in particular the jerk is quadratic in time.
- (4.1.3) When getting close to stopping, it would probably be sensible to optimise the stopping not just over the stopping time, but also over the stopping distance too. In the Kalman filter simulations, the largest 'corrections' are applied near the end. But provided a sufficient safety cushion is built into the initial stopping position, it doesn't matter if the car stops a few centimetres in front or behind that point. It's better to choose a smoother trajectory than be exactly in the right place.

4.2 Friction

- (4.2.1) Friction will, unfortunately, be a cause of a certain amount of jerk in some cases. Take a look at the example in Figures 8 and 9. Both friction and gravity are in the same direction when the block is moving uphill. When the block starts to stick onto the surface, the friction changes direction rapidly causing jerk. What this tells us is that in certain cases, trying to get the car to stop using the brake only may not work in all situations and that a more sophisticated control mechanism using the engine is necessary. However, the magnitude of the jerk can be reduced by a slower stop.

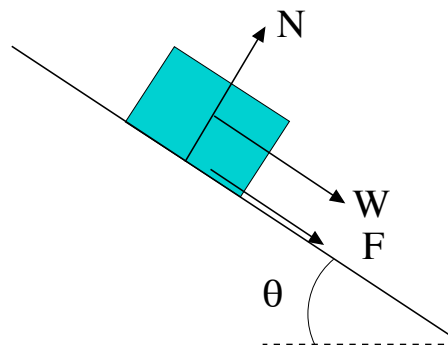


Figure 8: Uphill movement (sliding)

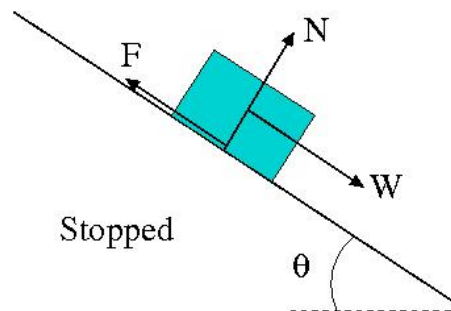


Figure 9: Uphill movement (stopped)

- (4.2.2) However, the sliding friction model should still be updated in the future if it is felt that the stick-slip boundary is the cause of some of the jerk. Stick-slip is caused by the surfaces alternating between sticking to each other and sliding over each other, with a corresponding change in the force of friction. Typically, the static friction coefficient between two surfaces is larger than the kinetic friction coefficient. If an applied force is large enough to overcome the static friction, then the reduction of the friction to the kinetic friction can cause a sudden jump in acceleration.

- (4.2.3) Andersson et al (6.1.1) recommend that where the final position is unimportant, one should use the combined Stribeck-tanh model. Where the final position is important, we should use a combined Stribeck-Dankowicz model. They note that the Coulomb model does not always represent behaviour in a contact set well but, other models are not much better and/or share the same problems as the Coulomb model hence the Coulomb model is still the preferred friction model by many.
- (4.2.4) They propose that the combined model suitable for ‘small’ displacements such as the Canudas de Wit model or the combined Coulomb, Stribeck, viscous and Dankowicz model should be used in many cases. Whilst analysis of other models is given, no conclusions are drawn as to whether these combined models are better. Their ability to model micro-slip and other effects for small displacements could make them relevant. The models can be seen in the Appendix in sections 5.4 and 5.5.
- (4.2.5) Finally, the jerk when the brakes ‘bite’ is almost inevitable. The key to minimizing this is to have an approach trajectory that means your velocity and acceleration are both getting as close to zero as possible at the same time (and hopefully somewhere near your desired stopping point).

4.3 Suggested further research

- (4.3.1) Further work would include stress tests using a simulation which is then followed by some real physical tests. It might be the case that the linear relationship between the brake pressure and the car acceleration might be a good enough model in reality and if not, this is when one could look into including a more sophisticated model for friction mentioned in sections 5.4 and 5.5.
- (4.3.2) To summarise, we constructed a control system that would be resistant to uncertainties (that is, uncertainties to the control system of the car) and that would in theory minimise the total jerk of the stopping procedure. Simple simulation results show that the acceleration and jerk levels are within the range of comfort specified by Jaguar Land Rover.

5 Appendix

5.1 Derivation of the Euler–Lagrange Equations

- (5.1.1) Consider a functional

$$I[v, \tau] = \int_0^\tau F(\ddot{v}, \dot{v}, v) dt \quad (24)$$

which we wish to minimise by varying the path $v(t)$ and the time interval τ , subject to the boundary conditions

$$v(0) = A, \quad \dot{v}(0) = B, \quad v(\tau) = C, \quad \dot{v}(\tau) = D. \quad (25)$$

(5.1.2) We consider variations $\delta v(t)$ and $\delta\tau$. To satisfy the boundary conditions, we find that the path variations must satisfy

$$\delta v(0) = 0, \quad \dot{\delta v}(0) = 0, \quad \delta\tau \dot{v}(\tau) + \delta v(\tau) = 0, \quad \delta\tau \ddot{v}(\tau) + \dot{\delta v}(\tau) = 0. \quad (26)$$

We define

$$\delta I = I[v + \delta v, \tau + \delta\tau] - I[v, \tau]. \quad (27)$$

Using integration by parts and applying the boundary conditions, we find that

$$\begin{aligned} \delta I = & \int_0^\tau \delta v \left[\frac{d^2}{dt^2} \left(\frac{\partial F}{\partial \ddot{v}} \right) - \frac{d}{dt} \left(\frac{\partial F}{\partial \dot{v}} \right) + \frac{\partial F}{\partial v} \right] dt \\ & + \delta\tau \left[F(\ddot{v}, \dot{v}, v) - \ddot{v} \frac{\partial F}{\partial \ddot{v}} - \dot{v} \frac{\partial F}{\partial \dot{v}} + v \frac{d}{dt} \left(\frac{\partial F}{\partial \ddot{v}} \right) \right]_{t=\tau} \\ & + O(\delta v^2, \dot{\delta v}^2, \ddot{\delta v}^2, \delta\tau^2). \end{aligned} \quad (28)$$

For a stationary point with respect to changes in v and τ , we therefore require that

$$\frac{d^2}{dt^2} \left(\frac{\partial F}{\partial \ddot{v}} \right) - \frac{d}{dt} \left(\frac{\partial F}{\partial \dot{v}} \right) + \frac{\partial F}{\partial v} = 0, \quad (29)$$

$$\left[F(\ddot{v}, \dot{v}, v) - \ddot{v} \frac{\partial F}{\partial \ddot{v}} - \dot{v} \frac{\partial F}{\partial \dot{v}} + v \frac{d}{dt} \left(\frac{\partial F}{\partial \ddot{v}} \right) \right]_{t=\tau} = 0. \quad (30)$$

5.2 Analysis of the optimisation problem (continued)

(5.2.1) The solution to the optimisation problem in section 2.1 is obtained by following the analysis continued in this section.

(5.2.2) The polynomials (11) minimise J between the initial and final conditions over the given time interval τ . We shall use them to construct solutions including the additional constraint $v \geq 0$, and allowing for optimisation with respect to variations in τ .

(5.2.3) The condition (10) to begin at a stationary point with respect to variations in τ is $\ddot{v}(\tau) = 0$ which implies $A = 0$. This gives a relationship between α and τ :

$$\alpha\tau^2 + 8\tau - 20 = 0. \quad (31)$$

(5.2.4) Examining figure 1, we see that for $\alpha > -4/5$ there are two values of τ satisfying (31). However, only the lower branch satisfies $v \geq 0$. (The polynomials in regions 3–6 have $v < 0$ for some values of t .) A check on the values of J for each of the solutions shows it is always in increasing

function of τ , so we might conclude¹ that for $\alpha > -4/5$, the minimising solution is the polynomial (11) with τ lying on the lower branch of (31), i.e.

$$\tau = \frac{5}{1 + \sqrt{1 + 5\alpha/4}}. \quad (32)$$

(5.2.5) For $\alpha < -4/5$ there are no polynomial solutions satisfying (31). Nevertheless, J is still an increasing function of τ , so it would be tempting to increase τ as much as possible before violating a constraint: either (a) $v \geq 0$ or (b) $\dot{v} \leq 0$. The former would put us on the upper boundary of region 7 ($v(t^*) = \dot{v}(t^*) = 0$), and the latter the upper boundary of region 8 ($\dot{v}(t^*) = \ddot{v}(t^*) = 0$).

(5.2.6) However, at the point in the trajectory where the constraint is only just satisfied, the Euler–Lagrange equations no longer apply.² We are allowed a discontinuity in \ddot{v} , and so we can switch from one polynomial solution to another. We conclude that the solution must involve following one polynomial solution until either (a) $v(t^*) = \dot{v}(t^*) = 0$ or (b) $\dot{v}(t^*) = 0$, $v(t^*) > 0$, and then switching to a different polynomial solution from that point on. In case (a), $\dot{v}(t)$ is continuous across the jump, so we must have $\dot{v}(t^*) = 0$ to prevent $v(t) > 0$ immediately after the jump. In case (b), since \ddot{v} can jump $\dot{v}(t) < 0$ can be avoided even if $\ddot{v}(t_-^*) \neq 0$.

(5.2.7) The total stopping distance (which is 1 with our non-dimensionalisation) must be partitioned as $1 = d_1 + d_2$ between the two phases of the motion, and the optimal polynomial found for each phase. We must then determine the optimal partition (d_1, d_2) and transition time t^* in order to minimise the total discomfort over both phases. Sketches of this partitioning showing the two phases of the motion are shown in figure 10.

(5.2.8) The first phase of the motion $0 < t < t^*$ involves getting from the initial conditions to a situation in which $\dot{v}(t^*) = 0$ with either (a) $v(t^*) = 0$ or with (b) $v(t^*) > 0$, in a distance $d_1 < 1$. These solutions can be related to the polynomials (11). In case (a), they are just the same polynomials but with α and τ redefined to take into account the shorter distance. (Decreasing the distance corresponds to decreasing the magnitude of α and increasing the magnitude of τ .) In case (b), we must also add a constant $v^* = v(t^*)$ to the polynomial to obtain the non-zero velocity at $t = t^*$.

(5.2.9) The second phase of the motion $t^* < t < \tau$ starts from $\dot{v}(t^*) = 0$, with $v(t^*) = 0$ in case (a) and $v(t^*) > 0$ in case (b). Again the optimal solutions

¹Actually, as we shall see below, this branch only applies for $\alpha > -3/4$.

²This is because we are unable to perform arbitrary deformations to the trajectory at that point, without violating the constraint.

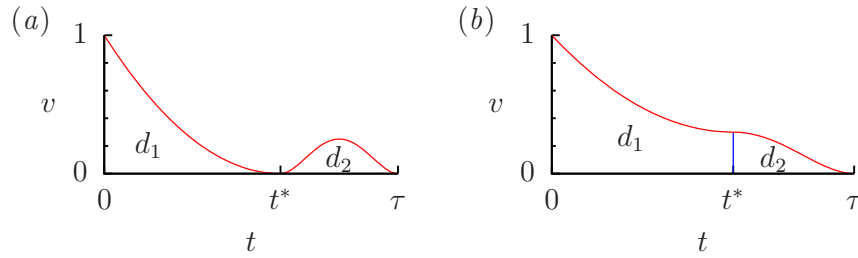


Figure 10: Sketches of possible split solutions in cases where one of the constraints is only just satisfied at a point $t = t^* \in (0, \tau)$. (a) with the constraint $v(t) \geq 0$, and (b) with the constraint $\dot{v}(t) \leq 0$. The paths must be optimised over variations in t^* , τ , d_1 , $d_2 = 1 - d_1$, and in case (b) $v^* = v(t^*)$.

can be related by a simple re-scaling to the polynomials (11). In case (a), the optimal solution for $t > t_0$ corresponds to a point on the red line in figure 1 with $\alpha = +\infty$. This solution takes an infinite time to cover the remaining distance by creeping forwards very slowly from the initial point of rest. While not particularly desirable physically, this solution makes no contribution to the jerk integral. In case (b) the optimal solution for $t > t^*$ corresponds to the point E on figure 1. This solution makes a positive contribution to J proportional to v^{*2} and is depicted in figure 4.

(5.2.10) In case (b) we see that, for a given (d_1, d_2) , the contribution to J from the second phase of the motion is minimised by taking $v(t^*)$ as small as possible. This is also found to be the case³ for the first phase of the motion. Hence case (b) is reduced to case (a).

(5.2.11) For case (a), the second phase of the motion makes no contribution to J , so it is just a matter of choosing the distance and time for the first phase to minimise J . This process is made easier by observing the behaviour of the Lagrange multiplier $\lambda = 48C$. When $\lambda < 0$, there exists a solution with a longer stopping distance and smaller J . When $\lambda > 0$ there exists a solution with a shorter stopping distance and smaller J . Provided d_1 doesn't exceed the total (non-dimensional) stopping distance of 1, the optimal solution therefore lies on the curve $\lambda = 0$. We find that the optimal trajectory corresponds to the point B on figure 1. The distance is given by $d_1 = -3/(4\alpha)$, so this is acceptable as long as $\alpha \leq -3/4$. This solution is depicted in figure 3.

We also find that this two-phase solution has a smaller value of J than the previously proposed single-phase solution for $-4/5 \leq \alpha < -3/4$, i.e. whenever $\lambda > 0$.

³Details omitted here.

(5.2.12) This leads us to the solution stated in paragraph (2.2.7).

5.3 An aside on self-similar stopping profiles

(5.3.1) We have seen that the solution from a given set of initial conditions that minimised the discomfort over a given stopping time depended on two non-dimensional parameters

$$\alpha = \frac{a_0 D}{v_0^2}, \quad \tau = \frac{v_0 T}{D}. \quad (33)$$

(5.3.2) At any point on an optimal stopping profile, we may examine the current conditions and re-calculate α and τ based on those conditions. The remainder of the trajectory we are about to follow would be returned as the optimal path for the new (α, τ) pair. It is therefore interesting to ask how α and τ evolve as we follow a stopping trajectory, and in particular if any trajectories (optimal or otherwise) are self-similar, in the sense that α and τ remain unchanged as the trajectory is followed.

(5.3.3) Suppose we follow the path $x(t) \leq 0$ to stop at $x = 0$. Then at any point on the trajectory, we have

$$\alpha = -\frac{\ddot{x}x}{\dot{x}^2}, \quad \tau = \frac{\dot{x}T}{x} \quad (34)$$

With α constant, we can integrate the first equation once to obtain

$$\dot{x} = C(-x)^{-\alpha}, \quad (35)$$

for some constant C . A second integration yields

$$x(t) = -C'|t - t_0|^{\frac{1}{1+\alpha}}, \quad (36)$$

where C' and t_0 are constants.

(5.3.4) There are now two possibilities:

(a) If $1 + \alpha > 0$ then we stop in a finite time, and $T = t_0 - t$. Substitution into (34b) yields the requirement

$$\tau = \frac{1}{1 + \alpha} \quad (37)$$

(b) Otherwise $1 + \alpha < 0$ and stopping takes an infinite time. Then $T = \infty$, and there is no additional requirement from (34b).

(5.3.5) The α - τ relation (37) for the self-similar solutions of type 1 is shown on figure 1. We note that the self-similar solutions have the position x as a power of t , and for integer values of τ the solution is a polynomial of order

τ . For $\tau > 2$ the self-similar solution also satisfies $v(\tau) = \dot{v}(\tau) = 0$. Hence for $\tau = 3, 4, 5$ the solution is a polynomial of order at most 5, which also satisfies the end-point boundary conditions. These three solutions therefore coincide with the optimal solutions (derived above) at those points.

(5.3.6) These three points (marked A, B and C on figure 1) are thus the only stationary points in the α - τ phase plane. It may be shown that, when following the optimal polynomial solutions, A $(-4/5, 5)$ is an unstable node, B $(-3/4, 4)$ is a saddle point, and C $(-2/3, 3)$ is a stable node.

(5.3.7) The evolution of α and τ for the optimal solutions described in section 2.2 is as follows. Case 1 solutions follow the red line in Figure 1 to the left and converge to point B as $t \rightarrow \tau$. Case 2 solutions remain at point B until the transition point.

5.4 Friction Models: Canudas de Wit Model

(5.4.1) Consider friction between two materials as contact between bristles. The bristles from one surface are rigid whilst the bristles on the other surface are flexible. Let the deflection, z , of bristles satisfy

$$\frac{dz}{dt} = v \left(1 - \frac{z}{g(v)} \right) \quad (38)$$

where v is the relative velocity between the two surfaces and $g(\cdot) > 0$ is a function dependant on the properties of the two materials such as temperature, lubrication *etc.*

(5.4.2) The friction force is described by

$$F = \sigma_0 z + \sigma_1 \frac{dz}{dt} + \sigma_2 v \quad (39)$$

where σ_0 represents stiffness, σ_1 is the damping coefficient and σ_2 is the viscous friction coefficient.

(5.4.3) The proposed form of $g(v)$ which describes the Stribeck effect (*i.e.* lubricated sliding contact friction decreases with increased sliding speed due to viscous and thermal effects.) is

$$\sigma_0 g(v) = F_c + (F_s - F_c) e^{\left(\frac{v}{v_s}\right)^2} \quad (40)$$

where F_c is the Coulomb friction, F_s is the maximum static friction and v_s is the Stribeck velocity.

5.5 Friction Models: Combined Coulomb, Stribeck, viscous, Dankowicz Model

- (5.5.1) From Dankowicz, take friction represented by a first order differential equation

$$\dot{z} = \dot{x} \left(1 - \frac{z\dot{x}}{\delta|\dot{x}|} \right) \quad (41)$$

where δ is the micro-slip displacement before the main slip. This parameter would have to be determined experimentally.

- (5.5.2) The combined model for friction takes the form

$$F = \left(1 + \left(\frac{F_s}{F_c} - 1 \right) e^{-(|\dot{x}|/v_s)^i} \right) F_c \frac{z}{\delta} + k_c \dot{x} \quad (42)$$

and allows for Coulomb, viscous, Stribeck and micro-slip effects. However all parameters, δ , i , v_s , F_c and F_s must be determined from dynamic friction tests.

6 Bibliography

6.1 Friction references

- (6.1.1) S. Andersson, A Söderburg, S. Sjörlund: Friction models for sliding dry boundary & mixed lubricated contacts - Tribology International, 40, (2007) 580-587

A reference for various friction models. They consider several friction models: Coulomb; viscous; Stribeck; combined models; models for small displacements; models to include stochastic nature of friction.

- (6.1.2) C. Canudas et al: A new model for control systems with friction - IEEE Transactions on automatic control v.40, no. 3 March 1995

Another reference for various friction models.